This article was downloaded by: [Institute Of Atmospheric Physics]
On: 09 December 2014, At: 15:34
Publisher: Taylor & Francis
Informa Ltd Registered in England and Wales Registered Number: 1072954 Registered office: Mortimer House, 37-41 Mortimer Street, London W1T 3JH, UK

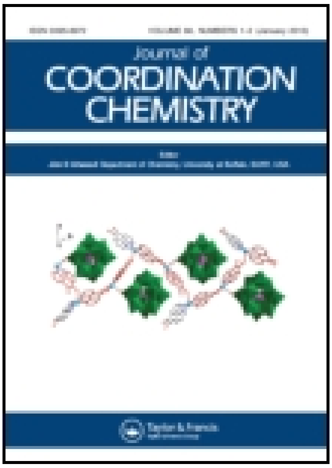

Click for updates

Journal of Coordination Chemistry
Publication details, including instructions for authors and subscription information:
http://www.tandfonline.com/loi/gcoo20

Two new coordination polymers based on N-heterocyclic carboxylic acids

Na Wang[ab], Xiao-Yang Yu[a], Xiao Zhang[c], Wei-Ping Gao[a], Rui Xin[ab], Hong Zhang[b], Yan-Yan Yang[a] & Xiao-Shu Qu[a]

[a] Jilin Institute of Chemical Technology, Jilin, PR China

[b] Department of Chemistry, Northeast Normal University, Changchun, PR China

[c] State Key Lab of Urban Water Resource and Environment (SKLUWRE) & Academy of Fundamental and Interdisciplinary Science, Harbin Institute of Technology, Harbin, PR China

Accepted author version posted online: 19 Mar 2014.Published online: 22 Apr 2014.

To cite this article: Na Wang, Xiao-Yang Yu, Xiao Zhang, Wei-Ping Gao, Rui Xin, Hong Zhang, Yan-Yan Yang & Xiao-Shu Qu (2014) Two new coordination polymers based on N-heterocyclic carboxylic acids, Journal of Coordination Chemistry, 67:5, 837-846, DOI: 10.1080/00958972.2014.905683

To link to this article: http://dx.doi.org/10.1080/00958972.2014.905683

PLEASE SCROLL DOWN FOR ARTICLE

Taylor & Francis makes every effort to ensure the accuracy of all the information (the "Content") contained in the publications on our platform. However, Taylor & Francis, our agents, and our licensors make no representations or warranties whatsoever as to the accuracy, completeness, or suitability for any purpose of the Content. Any opinions and views expressed in this publication are the opinions and views of the authors, and are not the views of or endorsed by Taylor & Francis. The accuracy of the Content should not be relied upon and should be independently verified with primary sources of information. Taylor and Francis shall not be liable for any losses, actions, claims, proceedings, demands, costs, expenses, damages, and other liabilities whatsoever or howsoever caused arising directly or indirectly in connection with, in relation to or arising out of the use of the Content.

This article may be used for research, teaching, and private study purposes. Any substantial or systematic reproduction, redistribution, reselling, loan, sub-licensing, systematic supply, or distribution in any form to anyone is expressly forbidden. Terms &

Journal of Coordination Chemistry, 2014
Vol. 67, No. 5, 837–846, http://dx.doi.org/10.1080/00958972.2014.905683

Two new coordination polymers based on N-heterocyclic carboxylic acids

NA WANG†‡, XIAO-YANG YU*†, XIAO ZHANG§, WEI-PING GAO*†, RUI XIN†‡,
HONG ZHANG*‡, YAN-YAN YANG† and XIAO-SHU QU†

†Jilin Institute of Chemical Technology, Jilin, PR China
‡Department of Chemistry, Northeast Normal University, Changchun, PR China
§State Key Lab of Urban Water Resource and Environment (SKLUWRE) & Academy of
Fundamental and Interdisciplinary Science, Harbin Institute of Technology, Harbin, PR China

(*Received 13 May 2013; accepted 9 January 2014*)

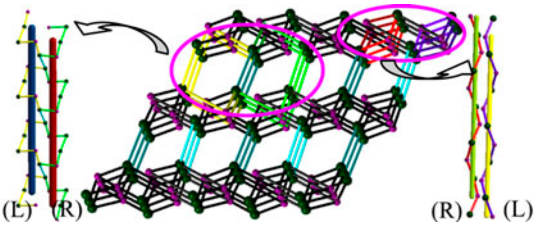

Two new coordination polymers, $[(Cu_2(o\text{-}HPIDC)_2(H_2O)_2]_n$ (**1**) and $\{[Nd(p\text{-}HPIDC)(ox)_{0.5}(H_2O)]\cdot 2H_2O\}_n$ (**2**) ($o\text{-}H_3PIDC$ = 2-(pyridinium-2-yl)-1H-imidazole-4,5-dicarboxylic acid, $p\text{-}H_3PIDC$ = 2-(pyridinium-4-yl)-1H-imidazole-4,5-dicarboxylic acid, H_2ox = oxalic acid), have been synthesized under hydrothermal. Compound **1** displays one-dimensional (1-D) infinite chains, which are stabilized by hydrogen bonds and $\pi\cdots\pi$ stacking interactions into a three-dimensional (3-D) supramolecular architecture. Compound **2** is a $(4\cdot 8^2)(4\cdot 8^5)$ 3-D network structure, and two pairs of single-left (L) and single-right-handed (R) helical chains can be found in the network. Thermogravimetric analyses of **1** and **2** are discussed in detail. In addition, the fluorescent property of **2** has been studied in the solid state at room temperature.

Two new coordination polymers, $[(Cu_2(o\text{-}HPIDC)_2(H_2O)_2]_n$ (**1**) and $\{[Nd(p\text{-}HPIDC)(ox)_{0.5}(H_2O)]\cdot 2H_2O\}_n$ (**2**) ($o\text{-}H_3PIDC$ = 2-(pyridine-2-yl)-1H-imidazole-4,5-dicarboxylic acid, $p\text{-}H_3PIDC$ = 2-(pyridine-4-yl)-1H-imidazole-4,5-dicarboxylic acid, H_2ox = oxalic acid), have been synthesized under hydrothermal conditions and characterized by elemental and thermogravimetric analyses (TGA), infrared spectroscopy, and single-crystal X-ray diffraction. In **1**, $o\text{-}HPIDC^{2-}$ ligands link Cu(II) centers into infinite 1-D chains that are stabilized by hydrogen bonds and $\pi\cdots\pi$ stacking interactions into a 3-D supramolecular architecture. In **2**, ox^{2-} ligands link the 2-D $[Nd(p\text{-}HPIDC)]_n$ layers into a $(4\cdot 8^2)(4\cdot 8^5)$ 3-D network structure featuring two pairs of left-handed and right-handed helical chains. TGA of **1** and **2** are presented. In addition, the fluorescence properties of **2** have been studied in the solid state at room temperature.

Keywords: Coordination polymers; N-heterocyclic carboxylic acids; Crystal structure; Fluorescence

---

*Corresponding authors. Email: yangyangyu0103@sohu.com (X.-Y. Yu); gwp1960@163.com (W.-P. Gao); zhangh@nenu.edu.cn (H. Zhang)

1. Introduction

Design and synthesis of coordination polymers or metal-organic frameworks (MOFs) have been given much attention due to their intriguing structures and wide potential applications in gas adsorption and separation [1], luminescence [2], sensor technology [3], magnetism [4], and catalysis [5]. In general, structural motifs of these compounds are closely related to the coordination geometry of the metal centers and the number of coordination sites provided by the ligands [6–8]. Fascinating architectures and applications have been reported for various coordination polymers based on rigid N-heterocyclic multicarboxylate ligands [9–24], especially 4,5-imidazole carboxylic acid and its analogs [10–24], which possess strong coordination ability and can have functionalities as hydrogen bond acceptors and donors, and π-conjugated systems for extending networks. The multidentate N-heterocyclic ligands, 2-(pyridine-2-yl)-1H-imidazole-4,5-dicarboxylic acid (o-H_3PIDC) and 2-(pyridine-4-yl)-1H-imidazole-4,5-dicarboxylic acid (p-H_3PIDC), possess 4,5-imidazoledicarboxylate and pyridyl groups, which can enhance coordination abilities. Both o-H_3PIDC and p-H_3PIDC may be bridging ligands because of their structural features. They provide multiple coordination points, two carboxylic acids, and three N-donors to construct MOFs with various bridging modes [17–24]. They can be hydrogen bond acceptors and donors to assemble various supramolecular structures, as they can be partially or fully deprotonated to generate species with different charges. The pyridine ring is connected to the imidazole ring through a C–C bond, so the two rings not only can rotate around the C–C bond but can also generate $\pi\cdots\pi$ stacking interactions to assemble the compound. Due to different positions of pyridine, o-H_3PIDC may chelate metal ions, while p-H_3PIDC may link metal ions into an extended network. Taking all these factors into consideration, we chose o-H_3PIDC and p-H_3PIDC as ligands and synthesized $[(Cu_2(o\text{-}HPIDC)_2(H_2O)_2]_n$ (**1**) and $\{[Nd(p\text{-}HPIDC)(ox)_{0.5}(H_2O)]\cdot 2H_2O\}_n$ (**2**). Compound **1** exhibits an infinite 1-D chain structure, which is stabilized by hydrogen bonds and $\pi\cdots\pi$ stacking interactions to form a 3-D supramolecular framework. Compound **2** has a $(4\cdot 8^2)(4\cdot 8^5)$ 3-D network, which is formed through ox^{2-} ligands combining with 2-D $[Nd(p\text{-}HPIDC)]_n$ layers; two pairs of left-handed and right-handed helical chains can be found in the network.

2. Experimental setup

2.1. *Materials and physical measurements*

All reagents were purchased commercially and used without purification. C, H, and N elemental analyses were performed on a Perkin-Elmer 2400 Elemental Analyzer. IR (KBr pellets) spectra were recorded from 4000 to 400 cm^{-1} using a Perkin-Elmer Spectrum One FT-IR spectrometer. Thermal behavior was studied by thermogravimetric analyses (TGA) on a Perkin-Elmer Thermal Analysis system under N_2 at a heating rate of 10 °C min^{-1}, from room temperature to 800 and 1000 °C for **1** and **2**, respectively. Fluorescence spectra were obtained using a Hitachi F7000 fluorescence spectrophotometer.

2.2. *Synthesis of 1 and 2*

2.2.1. Synthesis of $[(Cu_2(o\text{-}HPIDC)_2(H_2O)_2]_n$ (1). A mixture of $CuCl_2\cdot 2H_2O$ (0.3 mM, 0.0519 g), o-H_3PIDC (0.1 mM, 0.0260 g), and $H_3PW_{12}O_{40}\cdot nH_2O$ (0.03 mM, 0.1038 g) was dissolved in 10 mL of distilled water at room temperature and the pH of the mixture was adjusted to 4.0 with 1.0 M NaOH. The suspension was put in a Teflon-lined autoclave at 120 °C for 5 days. After slow cooling to room temperature, green, block-shaped crystals (0.0264 g, 33% yield based on *o*-H_3PIDC) were filtered and washed with distilled water. Elem. Anal. Calcd (%) for $C_{20}H_{14}Cu_2N_6O_{10}$: C, 38.40; H, 2.26; N, 13.44. Found (%): C, 37.91; H, 2.11; N, 13.12. FT-IR (KBr pellet, cm^{-1}): 3395w, 1684m, 1610w, 1558vs, 1497vs, 1464s, 1436m, 1381m, 1284m, 1128w, 1022w, 863m, 715m, 548m, 459w.

2.2.2. Synthesis of {[Nd(*p*-HPIDC)(ox)$_{0.5}$(H_2O)]·$2H_2O$}$_n$ (2). A mixture of Nd $(NO_3)_3 \cdot 6H_2O$ (0.1 mM, 0.0438 g), *p*-H_3PIDC (0.05 mM, 0.0117 g), and H_2ox (0.05 mM, 0.0063 g) was dissolved in 10 mL of distilled water at room temperature. The pH was then adjusted to 3.5 with 1.0 M NaOH. The resulting suspension was sealed into a Teflon-lined autoclave and heated at 150 °C for 5 days. Flaky pink crystals (0.0142 g, 60% yield based on *p*-H_3PIDC) were collected. Elem. Anal. Calcd (%) for $C_{11}H_{11}N_3NdO_9$: C, 27.90; H, 2.32; N, 8.87. Found (%): C, 28.08; H, 2.34; N, 8.56. FT-IR (KBr pellet, cm^{-1}): 3434m, 2050w, 2025vs, 1598vs, 1535w, 1480w, 1439m, 1386w, 1362m, 1162s, 1118w, 1076s, 982w, 949w, 860vs, 801w, 791w, 793w, 547s.

2.3. *X-ray crystallography*

Single-crystal X-ray diffraction data of **1** were collected at 293 K on an Agilent Technology SuperNova Eos Dual system with a (Mo) microfocus source ($\lambda = 0.71073$ Å) and focusing multilayer mirror optics. The data for **2** were collected at 293 K on a Rigaku R-AXIS RAPID IP diffractometer with Mo Kα radiation ($\lambda = 0.71073$ Å). The absorption corrections were performed empirically. The crystal structures were solved by Direct Methods and refined by full-matrix least squares on F^2 using SHELXTL-97 [25]. Anisotropic thermal parameters were applied to all non-hydrogen atoms. In both **1** and **2**, hydrogens attached to

Table 1. Crystal data and structure refinement parameters for **1** and **2**.

	1	**2**
Empirical formula	$C_{20}H_{14}Cu_2N_6O_{10}$	$C_{11}H_{11}N_3NdO_9$
Formula weight	625.45	473.47
Crystal system	Triclinic	Monoclinic
Space group	*P-1*	$P2_1/c$
a (Å)	9.0294(4)	8.2878(4)
b (Å)	9.3373(3)	15.1480(5)
c (Å)	13.6060(6)	11.6746(5)
α (°)	98.059(3)	90
β (°)	105.585(4)	90.868(4)
γ (°)	97.707(3)	90
V (Å^3)	1076.14(8)	1465.50(1)
Z	2	4
μ (mm^{-1})	2.052	3.599
D_c (g/cm^3)	1.930	2.146
R (int)	0.0351	0.0576
GOF on F^2	0.986	1.001
R_1[a] [$I > 2\sigma(I)$]	0.0412	0.0337
wR_2[b] [$I > 2\sigma(I)$]	0.0940	0.0525

[a] $R_1 = \sum||F_0| - |F_c||/\sum|F_0|$.
[b] $wR_2 = \sum\{w(F_0^2 - F_c^2)^2]/\sum[w(F_0^2)]^2\}^{1/2}$.

Table 2. Selected bond distances (Å) and angles (°) for **1** and **2**.

1			
Cu(1)–N(5)	2.009(3)	Cu(2)–O(10)$^{\#1}$	1.949(3)
Cu(1)–N(2)	2.025(3)	Cu(2)–N(1)	2.024(3)
Cu(1)–N(3)	2.027(4)	Cu(2)–N(6)$^{\#1}$	2.025(3)
Cu(1)–O(1W)	2.034(3)	Cu(2)–O(2W)	2.040(3)
Cu(1)–N(4)	2.155(3)	Cu(2)–O(1)	2.132(3)
N(5)–Cu(1)–N(2)	177.80(1)	O(10)$^{\#1}$–Cu(2)–N(1)	92.41(1)
N(5)–Cu(1)–N(3)	101.05(1)	O(10)$^{\#1}$–Cu(2)–N(6)$^{\#1}$	83.97(1)
N(2)–Cu(1)–N(3)	80.58(1)	N(1)–Cu(2)–N(6)$^{\#1}$	171.01(1)
N(5)–Cu(1)–O(1W)	84.96(1)	O(10)$^{\#1}$–Cu(2)–O(2W)	141.72(1)
N(2)–Cu(1)–O(1W)	92.87(1)	N(1)–Cu(2)–O(2W)	90.32(1)
N(3)–Cu(1)–O(1W)	147.08(1)	N(6)$^{\#1}$–Cu(2)–O(2W)	97.62(1)
N(5)–Cu(1)–N(4)	77.95(1)	O(10)$^{\#1}$–Cu(2)–O(1)	126.26(1)
N(2)–Cu(1)–N(4)	102.69(1)	N(1)–Cu(2)–O(1)	80.61(1)
N(3)–Cu(1)–N(4)	116.55(1)	N(6)$^{\#1}$–Cu(2)–O(1)	94.86(1)
O(1W)–Cu(1)–N(4)	96.37(1)	O(2W)–Cu(2)–O(1)	91.86(1)
2			
Nd(1)–O(3)$^{\#1}$	2.355(3)	Nd(1)–O(6)	2.459(3)
Nd(1)–O(2)$^{\#1}$	2.395(3)	Nd(1)–O(1W)	2.462(3)
Nd(1)–O(4)$^{\#2}$	2.436(3)	Nd(1)–O(5)$^{\#3}$	2.491(4)
Nd(1)–O(1)	2.439(3)	Nd(1)–N(1)	2.618(4)
O(3)$^{\#1}$–Nd(1)–O(2)$^{\#1}$	74.33(1)	O(6)–Nd(1)–O(1W)	74.33(1)
O(3)$^{\#1}$–Nd(1)–O(4)$^{\#2}$	77.91(1)	O(3)$^{\#1}$–Nd(1)–O(5)$^{\#3}$	78.09(1)
O(2)$^{\#1}$–Nd(1)–O(4)$^{\#2}$	152.08(1)	O(2)$^{\#1}$–Nd(1)–O(5)$^{\#3}$	76.30(1)
O(3)$^{\#1}$–Nd(1)–O(1)	128.87(1)	O(4)$^{\#2}$–Nd(1)–O(5)$^{\#3}$	100.92(1)
O(2)$^{\#1}$–Nd(1)–O(1)	126.54(1)	O(1)–Nd(1)–O(5)$^{\#3}$	145.89(1)
O(4)$^{\#2}$–Nd(1)–O(1)	70.54(1)	O(6)–Nd(1)–O(5)$^{\#3}$	65.11(1)
O(3)$^{\#1}$–Nd(1)–O(6)	128.01(1)	O(1W)–Nd(1)–O(5)$^{\#3}$	94.56(1)
O(2)$^{\#1}$–Nd(1)–O(6)	125.90(1)	O(3)$^{\#1}$–Nd(1)–N(1)	85.28(1)
O(4)$^{\#2}$–Nd(1)–O(6)	74.72(1)	O(2)$^{\#1}$–Nd(1)–N(1)	73.95(1)
O(1)–Nd(1)–O(6)	80.85(1)	O(4)$^{\#2}$–Nd(1)–N(1)	101.05(1)
O(3)$^{\#1}$–Nd(1)–O(1W)	146.83(1)	O(1)–Nd(1)–N(1)	63.43(1)
O(2)$^{\#1}$–Nd(1)–O(1W)	72.50(1)	O(6)–Nd(1)–N(1)	142.78(1)
O(4)$^{\#2}$–Nd(1)–O(1W)	135.16(1)	O(1W)–Nd(1)–N(1)	85.10(1)
O(1)–Nd(1)–O(1W)	73.16(1)	O(5)$^{\#3}$–Nd(1)–N(1)	148.88(1)

Note: Symmetry codes for **1**: $\#1 = x - 1,\ y - 1,\ z$, for **2**: $\#1 = x,\ -y + 1/2,\ z + 1/2$; $\#2 = -x + 1,\ y - 1/2,\ -z + 1/2$; $\#3 = -x,\ -y,\ -z + 1$.

N and O were located from difference Fourier maps and refined isotropically, while those attached to carbons were placed geometrically. The crystal data and structure refinement parameters for **1** and **2** are summarized in table 1, and selected bond lengths and angles are listed in table 2. Hydrogen bond lengths and angles are listed in table S1 (see online supplemental material at http://dx.doi.org/10.1080/00958972.2014.905683) and selected geometric parameters for the $\pi\cdots\pi$ interactions are listed in table S2.

3. Results and discussion

3.1. *Synthesis*

Compounds **1** and **2** were synthesized under hydrothermal conditions, which have proven useful for preparation of new metal-organic coordination polymers. The original goal was synthesis of a Cu-polyoxometallate compound, but **1** was isolated instead. When the synthesis was repeated with only $CuCl_2 \cdot 2H_2O$ and *o*-H_3PIDC as starting materials, just a small amount of an amorphous green precipitate was obtained. Thus, $H_3PW_{12}O_{40} \cdot nH_2O$ has some effect on the preparation processes for **1**.

3.2. *Crystal structure analysis*

3.2.1. [(Cu_2(*o*-HPIDC)$_2$(H_2O)$_2$]$_n$ (1). X-ray diffraction analysis revealed that **1** crystallizes in the triclinic space group *P-1* and forms a 1-D chain. The asymmetric unit consists of two crystallographically independent Cu(II) ions, two *o*-HPIDC^{2-}, and two coordinated waters. As shown in figure 1, Cu1 is five-coordinate with N2, N3, N4, and N5 from two different *o*-HPIDC^{2-} ligands and one water O1W. Cu2 is also five-coordinate with O1 and N1 from one *o*-HPIDC^{2-}, O10$^{\#1}$, and N6$^{\#1}$ from another *o*-HPIDC^{2-} and one water O2W. Five-coordinate complexes usually adopt trigonal bipyramidal (TBP), square pyramidal (SP), or intermediate coordination geometries [26]. The angular structural parameter $\tau = |\beta - \alpha|/60$ ($\tau = 0$ for ideal SP and 1 for ideal TBP), where α and β are the first and second largest coordination angles, has been reported as a quantitative tool to determine the extent to which five-coordination geometries are more TBP or SP [27]. The τ values for coordination around Cu1 and Cu2 are 0.512 and 0.488, respectively, confirming intermediate coordination geometries between TBP and SP. The N–Cu1–N chelate bite angles are 77.95° and 80.58°, and the N–Cu2–O chelate bite angles are 80.61° and 83.97°. The Cu–N [2.010(3)–2.154(3) Å] and Cu–O [1.948(3)–2.133(3) Å] distances compare well with those observed for previously reported |(DAP)(DMF)$_{0.5}$(H_2O)$_2$|[Cu(*p*-HPIDC)] (DAP = 1,3-diaminopropane; Cu–N, 1.928 (6)–2.035(7) Å; Cu–O, 2.033(8)–2.183(9) Å) and the mixed valent species |(MPL)$_{0.5}$(H_2O)$_8$| [$Cu^{II}_2Cu^{I}$((*p*-HPIDC))$_2$((*p*-H_2PIDC))] (MPL = morpholine; Cu–N, 1.967(7)–2.004(7) Å and Cu–O, 1.918(7)–2.308(7) Å) [22] and for other related five-coordinate Cu(II) complexes [28, 29]. In the IR spectrum of **1** (figure S1), the band at 1684 cm^{-1} indicates a protonated carboxylic acid. The *o*-HPIDC^{2-} ligands adopt μ_2-tetradentate bridging in which the pyridine-N and the *ortho* imidazole N chelate to Cu1 and another imidazole N and the *ortho* carboxylato O chelate to Cu2. Both Cu1 and Cu2 are linked into a 1-D chain with Cu1···Cu2 distances of 6.0476(7) and 6.0611(7) Å. The pyridine and imidazole rings in one *o*-HPIDC^{2-} ligand are coplanar owing to the N, N-chelating and N, O-chelating coordination. The dihedral angle between the planes of two neighboring *o*-HPIDC^{2-} ligands is 55.32°. In the 1-D zigzag chain {[Mn_2(*o*-HPIDC)$_2$(H_2O)$_4$]·2DMF}$_n$, synthesized by Li *et al.* [18(b)], the *o*-HPIDC^{2-} also adopts the same μ_2-tetradentate bridging mode as in **1**.

The non-covalent hydrogen bond and $\pi \cdots \pi$ interactions play important roles in stabilization of **1**. The coordinated waters (O1W and O2W) are hydrogen bond donors to link the uncoordinated carboxylic oxygens (O5$^{\#3}$ and O3$^{\#2}$) of the neighboring chains into a 2-D

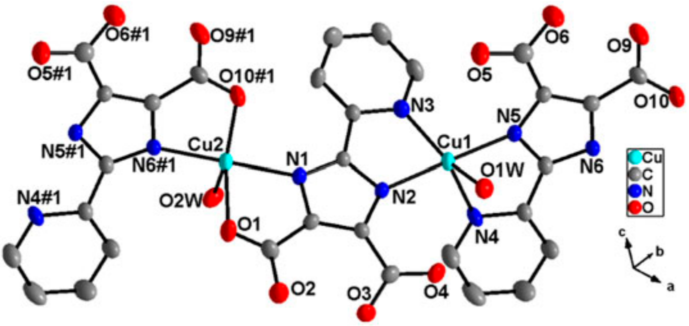

Figure 1. Structure of **1** with 50% probability thermal ellipsoids. Hydrogens are omitted for clarity. Symmetry code: #1 = $x - 1, y - 1, z$.

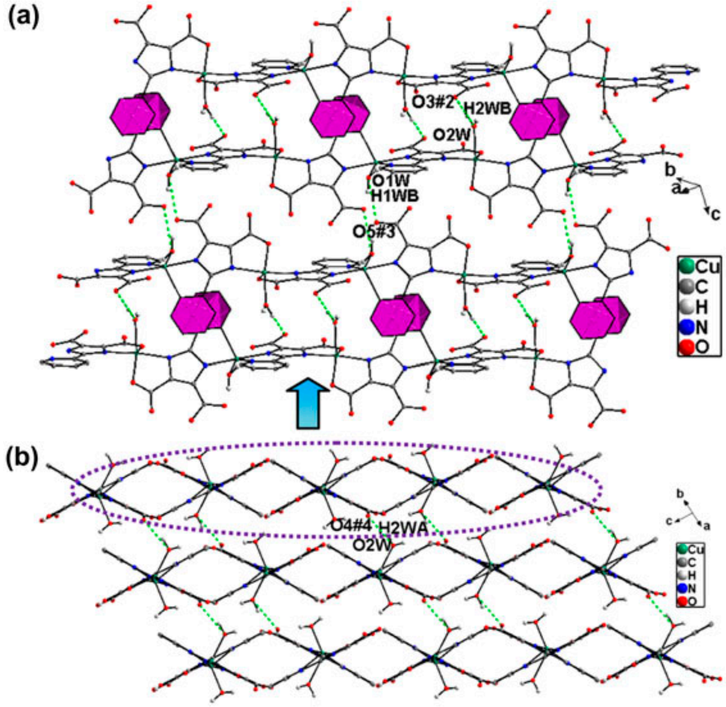

Figure 2. (a) Intermolecular hydrogen bonds link the adjacent 1-D chains into a 2-D layer. Weak $\pi \cdots \pi$ stacking interactions exist between pyridine rings (indicated in purple) in **1**. (b) Packing of 2-D layers of **1** to form a 3-D supramolecular network via intermolecular hydrogen bonds. Symmetry codes: #2 = $-x$, $-y$, $-z$; #3 = $-x+1$, $-y+1$, $-z+1$; #4 = $-x+1$, y, z (see http://dx.doi.org/10.1080/00958972.2014.905683 for color version).

supramolecular layer (table S1). Weak $\pi \cdots \pi$ stacking interactions (table S2) with a face-to-face distance of 3.504(2) Å between the pyridine rings further stabilize the 2-D supramolecular layer [figure 2(a)]. Neighboring 2-D supramolecular layers are further linked into a 3-D supramolecular network by hydrogen bonding between coordinated O2W and uncoordinated carboxylic O4$^{\#4}$ [figure 2(b)]. The non-covalent interactions possibly play an important role for constructing and stabilizing the 3-D supramolecular structure of **1**.

3.2.2. {[Nd(*p*-HPIDC)(ox)$_{0.5}$(H$_2$O)]·2H$_2$O}$_n$ (2). Compound **2** crystallizes in the monoclinic space group *P2$_1$/c*, and it is isostructural with {[Nd(μ_3-HPhIDC)(μ_2-C$_2$O$_4$)$_{0.5}$(H$_2$O)]·2H$_2$O}$_n$ (**3**, H$_3$PhIDC = 2-phenyl-1H-imidazole-4,5-dicarboxylic acid) reported by Chen [14(b)]. Besides a general structural description for **2**, we also make relevant comparisons of the structure of **2** with that of **3**. In **2**, Nd(III) is eight-coordinate by N1 and four oxygens (O1, O2$^{\#1}$, O3$^{\#1}$, and O4$^{\#2}$) from three *p*-HPIDC^{2-}, two oxygens (O5$^{\#3}$ and O6) from an oxalate, and one coordinated water (O1W), forming a distorted bicapped trigonal prism. The sets of atoms N1/O1W/O2$^{\#1}$ and O4$^{\#2}$/O5$^{\#3}$/O6 form the trigonal faces, and O1 and O3$^{\#1}$ are the two caps of the trigonal prism [figure 3(a) and (b)]. The bond angles around Nd(III) vary from 63.43(1)° to 152.08(1)°. The Nd–N [2.619(4) Å] and Nd–O [2.354(3)–2.491(4) Å, average, 2.434 Å] distances are similar to those for **3** (Nd–N, 2.661(4) Å; Nd–O, 2.344(3)–2.507(4) Å; average, 2.433 Å) [14(b)] and are comparable to

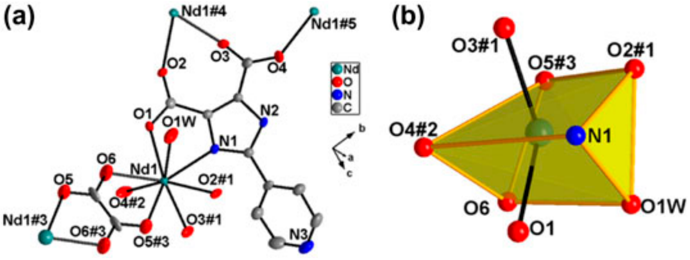

Figure 3. (a) Structure of **2** with 50% probability thermal ellipsoids. (b) The distorted bicapped trigonal prism environment of Nd1 in **2**. Hydrogens are omitted for clarity. Symmetry codes: #1 = x, $-y+1/2$, $z+1/2$; #2 = $-x+1$, $y-1/2$, $-z+1/2$; #3 = $-x$, $-y$, $-z+1$; #4 = x, $-y+1/2$, $z-1/2$; #5 = $-x+1$, $y+1/2$, $-z+1/2$.

those for eight-coordinate Nd(III) in |$(H_2O)_2$|[Nd_3(m-HPIDC)$_3$(m-PIDC)] (m-H_3PIDC = 2-(pyridine-3-yl)-1H-imidazole4,5-dicarboxylic acid) (Nd1–N, 2.601(4) Å; Nd–O, 2.359(4)–2.547(3) Å; average, 2.464 Å for Nd1–O and 2.425 Å for Nd2–O) [23]. The average Nd–O distance of the eight-coordinate Nd^{3+} in **2** is slightly shorter than the Nd–O distance in the nine-coordinate Nd^{3+} in |$(H_2O)_5(H_3O)(NO_3)$|[Nd_2(p-HPIDC)$_3$$(H_2O)_4$] (average, Nd1–O, 2.498 Å; Nd2–O, 2.519 Å) [23]. In the IR spectrum of **2** (figure S1), the absence of a band at 1700 cm^{-1} indicates deprotonation of the COOH to form COO$^-$. The p-HPIDC^{2-} ligands are μ_3-bridging to coordinate Nd(III) into a 2-D layer [figure 4(a)] using four carboxylate oxygens and one imidazole nitrogen through a μ_3-kO, kO$'$, O$''$: kO$'''$, N coordination [figure 3(a)]. Due to the uncoordinated pyridine N, the p-HPIDC^{2-} in **2** adopts the same coordination mode as μ_3-HPhIDC^{2-} in **3** [14(b)]. For p-HPIDC^{2-} in **2**, the pyridine and imidazole rings rotate around the C–C bond with a dihedral angle of 53.42°. There are also $\pi\cdots\pi$ stacking interactions between adjacent pyridine and imidazole rings of two neighboring p-HPIDC^{2-} ligands [figure 4(a), table S2]. Furthermore, ox^{2-} are μ_2-bridging to coordinate two neighboring Nd(III), linking 2-D layers into a 3-D network [figure 4(b)]. Four neighboring interstitial waters (O2W, O3W$^{\#1}$, O2W$^{\#6}$, and O3W$^{\#7}$) hydrogen bond to each other to form a water tetramer that links two coordinated waters (O1W and O1W$^{\#1}$) at the two diagonal vertices of a quadrilateral (figure S2). The average O···O distance of the water cluster is 2.90 Å, which is slightly longer than the reported 2.85 Å of liquid water [30]. If the p-HPIDC^{2-} ligands are considered as three-connected nodes and the ox^{2-} ligands as bridges, a schematic diagram (OLEX) shows that the Schläfli symbol for **2** is $(4\cdot 8^2)(4\cdot 8^5)$ [31]. There exist two pairs of left-handed (L) and right-handed (R) helical chains in the network [figure 4(c)].

3.3. *Thermogravimetric analyses*

TGA of **1** (figure S3) showed two main weight losses. The first of 4.92% from 83 to 154 °C is attributed to the release of two coordinated waters (Calcd 5.76%). Weight loss of 71.93% from 289 to 689 °C is attributed to decomposition and combustion of the ligands (Calcd 73.90%). The final decomposition product (23.15%) is CuO (Calcd 25.44%), which has been confirmed by a powder X-ray diffraction (PXRD) measurement. The peak positions of the recorded PXRD pattern are in agreement with the simulated pattern of CuO (figure S4). For **2**, a weight loss of 11.16% from 90 to 211 °C is attributed to release of the crystallization and coordinated water (Calcd 11.41%). Further weight loss from 410 to

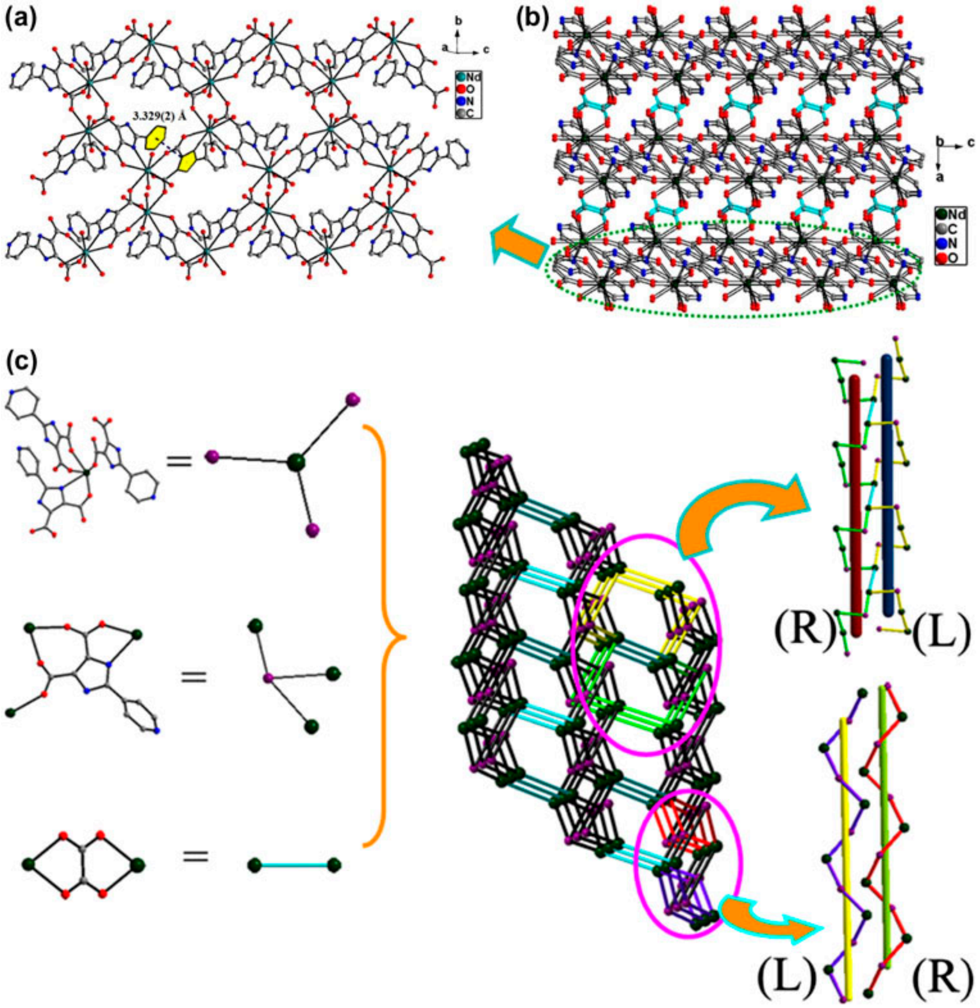

Figure 4. (a) The p-HPIDC^{2-} ligands coordinate Nd(III) into a 2-D layer with a $\pi \cdots \pi$ stacking interaction existing between adjacent pyridine and imidazole rings of two neighboring p-HPIDC^{2-} ligands. (b) Adjacent 2-D layers are bridged by ox^{2-} into a 3-D framework. (c) The 3-D $(4 \cdot 8^2)(4 \cdot 8^5)$ topological network in **2**, and the two pairs of left-handed (L) and right-handed (R) helical chains in the network. Hydrogens are omitted for clarity.

931 °C is due to decomposition and combustion of the ligands and the collapse of the framework. The final residual weight of 36.02% is consistent with that for Nd_2O_3 (Calcd 35.53%).

3.4. *Fluorescence properties of 2*

Considering the effect of organic constituents on the emission wavelengths and characteristic emission bands of Nd(III) compounds, the solid state fluorescence properties of p-H_3PIDC in the visible region [figure S5(a)] and **2** in visible region and in near-IR regions [figure S5(b)] were investigated. In the visible region, p-H_3PIDC exhibited blue photoluminescence with a single emission maximum at 452 nm ($\lambda_{ex} = 278$ nm) and **2** displayed an emission at 401 nm ($\lambda_{ex} = 345$ nm) with a blue shift of 51 nm. These emissions can probably be assigned to the intraligand (π–π^*) fluorescence emission, whereas the blue shift of **2** in comparison to *p*-H_3PIDC could be ascribed to metal–ligand interactions [23, 24]. When excited at 466 nm, **2** displayed three characteristic emission bands in the near-IR region (800−1700 nm), which are in agreement with previously reported Nd(III) complexes $[NdZn(imdc)(ip)(H_2O)_2]\cdot 3H_2O$ (H_3imdc = imidazole-4,5-dicarboxylic acid; ip = isophthalate) [15] and $Na[Nd_3(H_2O)_4(C_2O_4)_4(CH_3PO_3)]\cdot 2H_2O$ [32]. The three bands at 895, 1058, and 1328 nm can be attributed to the $^4F_{3/2}$-$^4I_{9/2}$, $^4F_{3/2}$-$^4I_{11/2}$, and $^4F_{3/2}$-$^4I_{13/2}$, respectively; the peak at 1058 nm is the strongest.

4. Conclusion

Two new compounds were synthesized by hydrothermal reactions and the structures were determined by single-crystal X-ray diffraction. Compound **1** has an infinite 1-D chain structure and the chains are further self-assembled into a 3-D supramolecular structure. Compound **2**, isoelectronic with **3**, has a 3-D MOF with $(4\cdot 8^2)(4\cdot 8^5)$ topology, and there simultaneously exist two pairs of left-handed (L) and right-handed (R) helical chains in the network. TGA of the two compounds and the fluorescence properties of **2** were also investigated.

Supplementary material

Figures of the hydrogen bond interactions of the water molecules in **2;** TGA curves for **1** and **2;** PXRD pattern of the final CuO residue from the decomposition of **1**; fluorescence spectra of *p*-H_3PIDC and **2**; FT-IR spectra of **1** and **2**; tables of hydrogen bond distances and angles and geometric parameters of the π–π stacking interactions. Crystallographic data reported in this article have been deposited with the Cambridge Crystallographic Data Center as supplementary publication (CCDC numbers are 930606 and 930607). This data can be obtained free of charge via http://www.ccdc.cam.ac.uk/conts/retrieving.html (or from the Cambridge Crystallographic Data Center, 12 Union Road, Cambridge CB2 1EZ, UK; Fax: +44 1223 336 033; E-mail: deposit@ccdc.cam.ac.uk).

Funding

The work is supported by Technology Research Program for Department of Education of Jilin Province [grant number 2012291]; the National Natural Science Foundation [grant number 51108122]; Open Project of State Key Laboratory of Urban Water Resource and Environment, Harbin Institute of Technology [grant number QA201025]; the Fundamental Research Funds for the Central Universities [grant number HIT. NSRIF. 2010053]; Science and Technology Innovation Talents Special Foundation of Harbin [grant number 2010RFQXG035], [grant number 2007RFXXG018].

References

[1] M. Dincă, J.R. Long. *J. Am. Chem. Soc.*, **127**, 9376 (2005).
[2] H.J. Tracy, J.L. Mullin, W.T. Klooster, J.A. Martin, J. Haug, S. Wallace, I. Rudloe, K. Watts. *Inorg. Chem.*, **44**, 2003 (2005).
[3] B.V. Harbuzaru, A. Corma, F. Rey, P. Atienzar, J.L. Jordá, H. García, D. Ananias, L.D. Carlos, J. Rocha. *Angew. Chem.*, **120**, 1096 (2008).
[4] S.M. Humphrey, P.T. Wood. *J. Am. Chem. Soc.*, **126**, 13236 (2004).
[5] M.J. Vitorino, T. Devic, M. Tromp, G. Férey, M. Visseaux. *Macromol. Chem. Phys.*, **210**, 1923 (2009).
[6] H.W. Kuai, J. Fan, Q. Liu, W.Y. Sun. *CrystEngComm*, **14**, 3708 (2012).
[7] Z.Y. Li, J.W. Dai, N. Wang, H.H. Qiu, S.T. Yue, Y.L. Liu. *Cryst. Growth Des.*, **10**, 2746 (2010).
[8] X. Han, X. Wang, G. Jin, X. Meng. *J. Coord. Chem.*, **66**, 800 (2013).
[9] X.Q. Zhao, B. Zhao, W. Shi, P. Cheng. *CrystEngComm*, **11**, 1261 (2009).
[10] Z.X. Wang, Q.F. Wu, H.J. Liu, M. Shao, H.P. Xiao, M.X. Li. *CrystEngComm*, **12**, 1139 (2010).
[11] Y. Wei, Y. Yu, R. Sa, Q. Li, K. Wu. *CrystEngComm*, **11**, 1054 (2009).
[12] Y.Q. Sun, G.Y. Yang. *Dalton Trans.*, 3771 (2007).
[13] N. Chen, J. Zhang, Y.C. Gao, Z.L. Yang, H.J. Lu, G. Li. *J. Coord. Chem.*, **64**, 2554 (2011).
[14] (a) M. Guo, N. Chen, Y.C. Gao, H.J. Lu, G. Li. *J. Coord. Chem.*, **65**, 1724 (2012); (b) N. Chen, Y. Zhang, Z.-L. Yang, G. Li. *J. Coord. Chem.*, **65**, 1221 (2012); (c) D.-P. Wang, Y.-G. Chen, H.-Y. Wang, C.-J. Zhang, Q. Tang. *J. Coord. Chem.*, **64**, 2824 (2011).
[15] S.-T. Yue, Z.-Q. Wei, N. Wang, W.-J. Liu, X. Zhao, L.-M. Chang, Y.-L. Liu, H.-H. Mo, Y.-P. Cai. *Inorg. Chem. Commun.*, **14**, 1396 (2011).
[16] R.S. Zhou, J.F. Song, Y.B. Li, C.Y. Xu, X.F. Yang. *Z. Anorg. Allg. Chem.*, **637**, 251 (2011).
[17] W. Zheng, Y. Wei, C. Tian, X. Xiao, K. Wu. *CrystEngComm*, **14**, 3347 (2012).
[18] (a) X. Li, B. Wu, R. Wang, H. Zhang, C. Niu, Y. Niu, H. Hou. *Inorg. Chem.*, **49**, 2600 (2010); (b) X. Li, W. Liu, B.-L. Wu, C.-X. Nian, H.-Y. Zhang. *Synth. React. Inorg. Met. Org. Chem.*, **42**, 231 (2012).
[19] X. Li, B.L. Wu, C.Y. Niu, Y.Y. Niu, H.Y. Zhang. *Cryst. Growth Des.*, **9**, 3423 (2009).
[20] S.Q. Zhang, F.L. Jiang, M.Y. Wu, R. Feng, J. Ma, W.T. Xu, M.C. Hong. *Inorg. Chem. Commun.*, **14**, 1400 (2011).
[21] L. Sun, G.Z. Li, M.H. Xu, X.J. Li, J.R. Li, H. Deng. *Eur. J. Inorg. Chem.*, **2012**, 1764 (2012).
[22] X. Jing, L. Zhang, T. Ma, G. Li, Y. Yu, Q. Huo, M. Eddaoudi, Y. Liu. *Cryst. Growth Des.*, **10**, 492 (2010).
[23] X. Jing, H. Meng, G. Li, Y. Yu, Q. Huo, M. Eddaoudi, Y. Liu. *Cryst. Growth Des.*, **10**, 3489 (2010).
[24] G. Yuan, K.Z. Shao, D.Y. Du, X.L. Wang, Z.M. Su, J.F. Ma. *CrystEngComm*, **14**, 1865 (2012).
[25] G.M. Sheldrick. *Acta Crystallogr., Sect. A*, **64**, 112 (2008).
[26] L. Sacconi. *Pure Appl. Chem.*, **17**, 95 (1968).
[27] A.W. Addison, T.N. Rao. *J. Chem. Soc., Dalton Trans.*, 1349 (1984).
[28] L.F. Ma, X.K. Huo, L.Y. Wang, J.G. Wang, Y.T. Fan. *J. Solid State Chem.*, **180**, 1648 (2007).
[29] Y. Qiu, K. Wang, Y. Liu, H. Deng, F. Sun, Y. Cai. *Inorg. Chim. Acta*, **360**, 1819 (2007).
[30] D.S. Eisenberg, W. Kauzmann. *The Structure and Properties of Water*, Oxford University Press, New York, NY (1969).
[31] J.V. Smith. *Am. Mineral.*, **63**, 960 (1978).
[32] Y.L. Huang, M.Y. Huang, T.H. Chan, B.C. Chang, K.H. Lii. *Chem. Mater.*, **19**, 3232 (2007).